

Late Quaternary dune accumulation along the western margin of South Africa: distinguishing forcing mechanisms through the analysis of migratory dune forms

Brian M. Chase^{a,b,*}, David S.G. Thomas^a

^a *Oxford University Centre for the Environment School of Geography, University of Oxford, Dyson Perrins Building, South Parks Road, Oxford, OX1 3QY, UK*

^b *Environmental and Geographical Science Department University of Cape Town, Private Bag, Rondebosch, 7701, South Africa*

Received 16 June 2006; received in revised form 31 August 2006; accepted 4 September 2006

Available online 24 October 2006

Editor: M.L. Delaney

Abstract

The west coast of South Africa is situated at a critical location between temperate and subtropical oceanic and atmospheric circulation systems, and palaeoenvironmental proxies from this region have the potential to elucidate issues concerning variations within these systems over glacial–interglacial cycles. While semi-arid climates have hindered the preservations of organic proxies, a variety of aeolian bedforms have been analysed in an effort to improve our understanding of environmental change in the region. Optically stimulated luminescence measurements of 51 samples from 15 reticulate dune sites along the west coast have enabled the identification of phases of aeolian activity, as well as periods of relative geomorphic stability. Combined with data derived from previous studies of the region's sediment accumulating deposits and other palaeoenvironmental proxies, periods of increased windiness are identified at 16–24, 30–33, 43–49 and 63–73 ka. From approximately 17–12 ka, decreasing transport capacity resulted in the stabilisation of the west coast's dune fields. During the Holocene Altithermal (~4–8 ka), despite reduced wind strength, increased aridity resulting from higher temperatures and a reduced influence of moisture bearing westerly systems appears to have triggered widespread remobilisation of the region's dune fields. The combination of ages from a variety of dune forms with different development mechanisms, and comparisons with a range of proxy data sources, have allowed for an enhanced interpretation of the region's aeolian archives, moving beyond simple correlations between dune activity and “aridity.”

© 2006 Elsevier B.V. All rights reserved.

Keywords: Quaternary palaeoenvironmental change; wind strength; aeolian proxies; luminescence dating; South Africa; Southern Hemisphere

1. Introduction

Compared to the Northern Hemisphere, our understanding of how Southern Hemisphere climate systems have reacted to the periods of global warming and cooling registered in ice and marine cores is still relatively poor [1]. Although it is clear that large, rapid temperature changes have occurred during the last glacial–interglacial

* Corresponding author. Tel.: +44 27 21 650 2873/4; fax: +44 27 21 650 3791.

E-mail address: brian.chase@ouce.ox.ac.uk (B.M. Chase).

cycle [2,3], we have only limited, and often imprecise, knowledge of how the major moisture-bearing atmospheric circulation systems have reacted to these changes, and how regional environments have been impacted.

A critical region for studying Southern Hemisphere climate and circulation dynamics is the western coast of southern Africa. This region is a transition zone between temperate and tropical systems and is thought to have experienced phases of significant environmental change resulting from variations in hemispheric circulation patterns [4].

The environmental history of west coast of southern Africa, however, remains largely unknown. This is due to a combination of the limited preservation potential offered to palaeoecological material by predominantly arid conditions north of Cape Town, limited research investigation, the remoteness of the area, and the relative paucity of closed sites suitable for preservation, such as coastal caves and rock shelters [e.g. 5]. As such, very few well-dated terrestrial palaeoecological records from the last glacial period have been recovered from the 2000 km western margin of South Africa and Namibia [6–10]. In lieu of terrestrial palaeoecological records, a variety of marine cores [11–14] and sedimentological records [15–17] have been analysed, but interpretations of their significance vary and have often been contradictory [18].

This paper reports findings from a luminescence dating programme that has investigated the potential of aeolian land forms as palaeogeomorphological climate proxies along the west coast of South Africa from 29°14'S to 33°00'S, the modern sub-humid to hyper-arid transition zone. In this zone, aeolian sediments are extremely common, in the form of sand dune systems that extend up to 60 km inland from the modern coastline. Like the dunes of the Namib Sand Sea to the north, the west coast dunes are not generally coastal dunes *per se*, but represent extensive continental dune systems that have the potential to provide important information on climatic and environmental conditions during phases of accumulation during the late Quaternary.

Previous studies by Chase and Thomas [19] of the west coast's coversand [c.f. 20–22]¹ deposits analysed

35 samples obtained from six dune cores. Results showed a strong correlation between aeolian accumulation and periods of enhanced humidity and windiness within the last glacial phase (~115–12 ka). Conditions during these periods were generally marked by increased hemispheric temperature gradients and invigorated global circulation systems [23,24]. Evidence from marine core records indicate wetter and windier conditions at these times [12–14], and charcoal records from the southern west coast in the Elands Bay region [25] suggest significantly more humid environments during the Last Glacial Maximum (LGM). This combination of wetter and windier conditions together with increased aeolian activity has been interpreted as indicative of west coast dune development being the result of increased wind energy and reinforced by fluvial sediment supply [19], rather than increased aridity as is commonly suggested for the interior dune systems of southern Africa [26–29].

A further phase of accumulation occurred during the Holocene Altithermal (HA, ~4–8 ka), yet marine records indicate decreased windiness at this time [13,14] and it is unlikely that increased transport capacity alone could account for dune development at this time. Only a very few Holocene ages were obtained from the west coast coversands, however, and it remains unclear whether aeolian activity during the HA was a function of regional climate change or simply local-scale reactivations.

To address this question, and better understand the nature of environmental change along the west coast, sediments from shallow reticulate dunes have been sampled for optically-stimulated luminescence (OSL) dating and analysis. While the region's coversands are primarily accumulatory in nature, with deposition generally outweighing deflation and erosion [30], the reticulate dunes have developed in areas where wind strength exceeds available sediment supply, and are broadly migratory forms. This question of sediment balance is critical to the correct interpretation of OSL ages from dunes. While mobile, the sediment in the reticulate dunes is cycled through the dune body, and in the process is regularly exposed to sunlight, bleaching the grains and removing their accumulated luminescence signal. As opposed to accumulatory coversand deposits, OSL ages from which are believed to indicate periods of aeolian activity, clusters of OSL ages from migratory reticulate dune forms indicate the termination of aeolian activity and the cessation of the recycling process. By providing an alternative but complementary perspective on the timing of aeolian activity, these fundamental differences in wind and sediment dynamics can be used to determine not only whether palaeo-wind fields were weakening or

¹ Though often related to higher latitude periglacial landscapes [22,23], the definition of coversands has been expanded [21] to encompass bodies of aeolian sand with low undulating relief, but little to no recognisable dune morphology. These are distinct from sand sheets in terms of particle size and dynamics of deposition. Coversands are interpreted as representing once active, perhaps significantly more expansive, dunefields. Their preservation may result from a combination of factors including topographic position, subsequent environmental conditions, and the amount of sediment deposited.

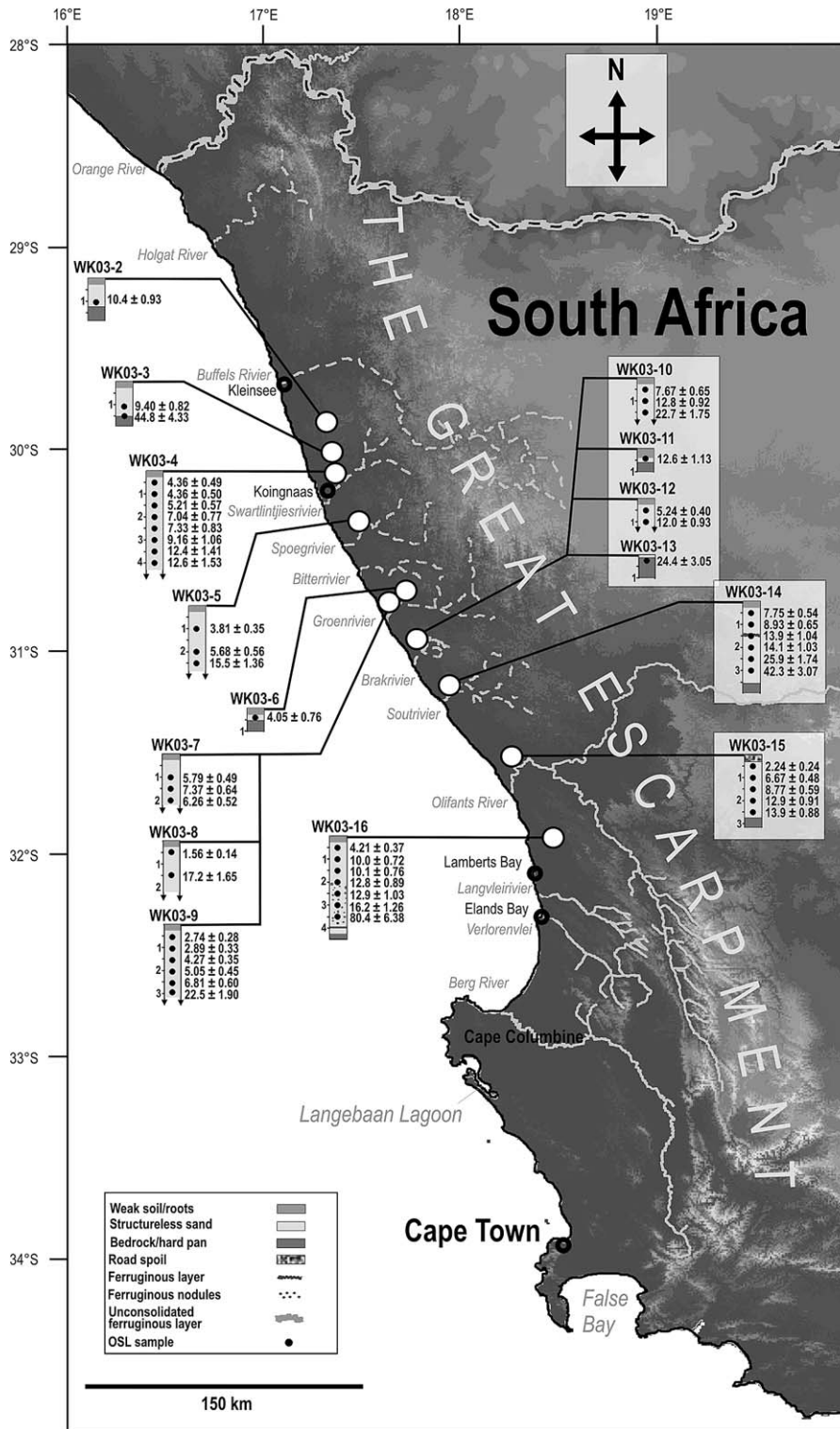


Fig. 1. Schematic diagram of the west coast of South Africa with sampling sites, stratigraphies and OSL ages shown.

intensifying, but also, and perhaps more importantly, the relative influence of the dominant controls of aeolian activity over time. With these data it is possible to more clearly identify past variations of vegetation/precipitation and sediment supply, and thus draw more reliable palaeoenvironmental interpretations.

2. Study area

The west coast of South Africa is characterized by a low relief plain extending from the mountains of the Great Escarpment in the east to the Atlantic Ocean in the west (Fig. 1). As the southernmost extension of the Namib Desert, the region is sometimes referred to as the Namaqualand Sandy Namib [31], or locally as the Sandveld. In the vicinity of Cape Columbine the coastal plain is up to 60 km wide, while in the central and northern regions it ranges from ~20–40 km wide, and is divided into a narrow coast marginal plain and a broader inland plateau situated at ~130–200 m a.p.s.l. Although much of the low-lying coastal margin plain exhibits a complex suite of Cenozoic deposits representing a range of littoral sedimentary environments [32], the interior plateau is characterized by deeply weathered bedrock (granites of the Namaqualand Metamorphic system [33]) covered by shallow aeolian sands.

2.1. Aeolian deposits of the central west coast

The distribution and depth of aeolian deposits along the central west coast is primarily a function of topography and the proximity and productivity of sediment sources. Over much of the exposed low-relief interior plateau, aeolian sediments are often only 20–50 cm in depth. In topographically-sheltered depressions, on lee slopes, or adjacent to fluvial source areas aeolian deposits can, however, exceed 8–10 m in depth.

Where aeolian material has accumulated, two general styles of deposition have occurred: deep, stacked coversand sequences in isolated locations sheltered from prevailing winds [described in 19], and reticulate dunes in shallow depressions found on the interior plateau. The latter is most prevalent, with reticulate dunefields usually between 50 and 150 km² in size, and composed of low (~1–4 m high) dune forms (Fig. 2). The complex patterning of bedforms that characterise these dune fields appear to be the product of at least two distinct wind regimes, one, predominantly unimodal, resulting in the emplacement of a base set of crescentic dune forms, and another, bimodal, resulting in the development of distinct linear elements through a process of reworking and elongation [34,35]. Presently, these dunes are well-vege-

tated but with only very weak soil development, a situation similar to that of the region's coversand deposits. The reticulate dune fields also exhibit a substantial

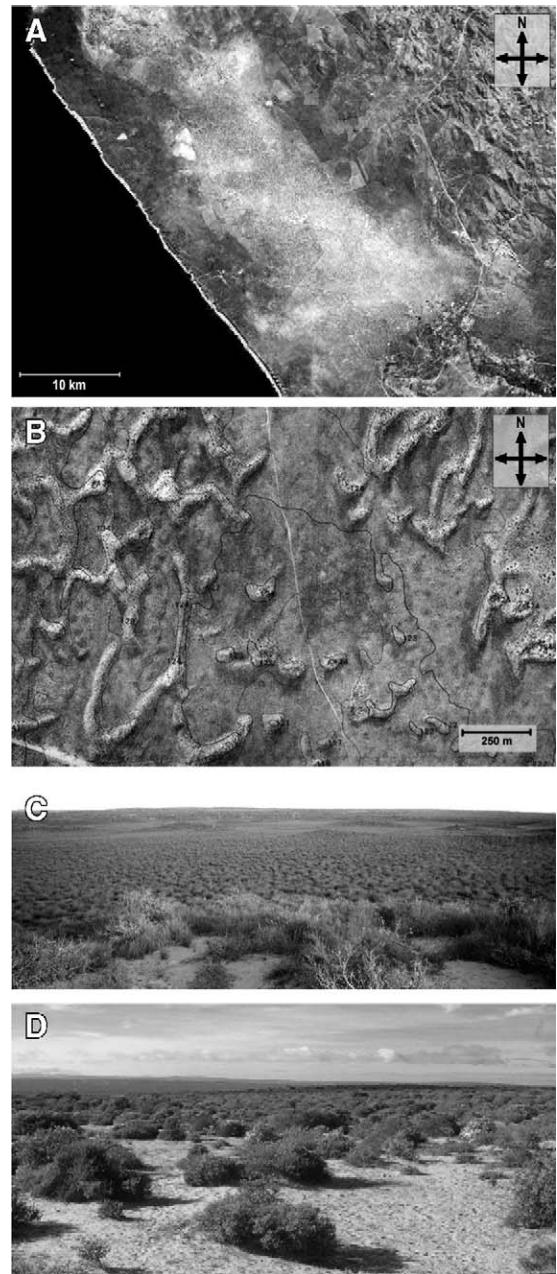


Fig. 2. Landscapes of the west coast of South Africa. A) Landsat 7 ETM+ image of the large reticulate dune field north of the Olifants River. B) Orthophoto of WK03-5 dunefield with sample site indicated. Note the variety of forms exhibited, from crescentic (bottom left) to quasi-linear (right). C) View east over the WK03-10–WK03-13 dunefield. D) View northwest over WK03-3 landscape, typical of upland areas of the coastal margin's interior plateau.

number of nebkhas scattered between the crescentic and reticulate forms.

3. Sampling and dating

The reticulate dune fields of the west coast were sampled along a 300 km north – south transect from the Brandberg Massif to Elands Bay (Fig. 1). By sampling extensively throughout the west coast reticulate dune systems, the aim was to identify regional patterns of sediment accumulation and dune development, allowing robust conclusions to be drawn concerning the timing and spatial extent of environmental conditions favouring dune development and preservation in the context of atmospheric and oceanic circulation dynamics. To better understand dunefield dynamics, a small number of samples were also taken from a selection of surficial interdune sands, as well as the sandy soils that have developed on the underlying bedrock.

3.1. Sampling procedure

A series 15 sites from the west coast's eight major reticulate dune systems were identified and sampled for this study (Table 1). Sites within each dunefield were generally selected to sample dune forms of sufficient size to provide the largest number of samples possible. At some locations, smaller dunes and interdune deposits were sampled as well in an effort to gain a broader range of information from the variety of sediments present within the dunefields. All dunes were sampled at identifiable crests, minimising the potential of dating samples that were perhaps deposited as a result of degradational processes such as sheet wash [36], rather than the aggradational processes that are implicit in common interpretations. At each site samples were collected in a vertical sequence using a Dormer™ hydraulic auger, with samples for luminescence dating taken at 50 cm intervals. Given the disruptive action of the auger, this was determined to be the maximum resolution possible with the equipment employed. While non-continuous sampling always introduces the possibility that periods of accumulation may be missed, the use of an auger allows for the sampling of the entire sediment body, something that is rarely achievable with other equipment in soft sediments [37,38]. This was deemed as a critical component of sample collection, as the questions being asked relate to the inception of dune stabilisation, and thus requires the retrieval of near-basal sediments.

Samples were taken with a 10-cm diameter hollow stainless steel sampling head that was lowered into the

core hole, being careful not to disturb the sides and contaminating the sample with younger sediment. A slide hammer then used to force the sampling head into the bottom of the core hole, packing the tube with sediment. The sample was then removed from the core and quickly placed in a lightproof bag, where the luminescence sample could be safely extracted by twisting a lightproof tube into the sampling head and removing the well-packed sediment. Samples taken from interdune deposits and surficial sands and soils were excavated using a spade to remove either shallow sediments or those that either not be penetrated by the auger. Sampling depth varied depending on the depth of the deposits and the limit to which the sections could be excavated.

3.2. Sedimentology

In general, the aeolian deposits of the west coast provide little stratigraphic evidence that could give clues to their history and evolution. While this observation is to some extent the result of the auguring action of the sampling equipment employed, similar situations of homogeneous, apparently unstratified dunes deposits have been reported in the Kalahari as well [39,40].

Sediments from most of the sampled reticulate dunes are dominated by medium-coarse sand, with a limited degree of variability both within and between sites. Mean grain size averages $1.8 \pm 0.14 \phi$, while the clay and silt fractions range from 3.5–7.5% by mass, with an average of 4.8% for all samples. Notable exceptions are samples from sites WK03-14 and WK03-16, which have significantly greater proportions of fines, ranging from 8.1–26.1% and 12.5–43.5% of the sample mass respectively (Fig. 3). Whereas most dunes from the west coast consist of entirely unstratified sand, both of these cores contained a unit of notably more consolidated sand. In the generally siltier WK03-16 core, while the degree of sediment compaction/cementation was distinct, there was little discernible difference in terms of sediment colour or grain size distribution relating to this layer. In WK03-14, however, the uppermost metre of sediment is similar to other west coast dune sands, with the consolidated unit marking a distinct boundary in terms of both sediment colour and grain size (Figs. 1 and 7).

3.3. Luminescence measurement details

Samples for OSL dating were prepared for measurement under subdued red light conditions. Carbonates and organic matter were removed using 10% HCl and 30% H₂O₂. Samples were then wet sieved to 180–212 μm or 212–250 μm depending on the most abundant

Table 1
Site locations and descriptions

Site (m)	Location	Altitude (a.s.l.)	Description
WK03-2	29.8369°S, 17.2697°E	194	3.5 (km) W of the Brandberg massif, 16 (km) from the coast. Low (1.25 (m) high) reticulate features on the eastern margin of the 20 (km) long Koingnaas aeolian deflation zone. Sampled to 1.25 (m) depth where a hard silty sand surface was encountered.
WK03-3	29.9933°S, 17.2928°E	253	17 (km) S of WK03-2, 12 (km) from the coast. 1.5 (m) sand mantle lying situated on the crest of a low hill separating the interior plateau from the coastal plain. Sampled to 1.5 (m) depth where a hard pan surface was encountered. Core was excavated a further 0.5 (m) with a spade to sample the underlying silty sand.
WK03-4	30.0928°S, 17.3122°E	155	10.7 (km) S of WK03-3, 11.8 (km) N of the Swartlinterivier, 12 (km) from the coast. Thick (+4 (m)), degraded transverse/barchanoid features developed in the lee of the upland of WK03-3. Sampled to 4 (m) depth at which point the core collapsed due to excessively dry sediment.
WK03-5	30.3350°S, 17.4225°E	133	29 (km) S of WK03-4, 3.6 (km) N of the Spoegrivier, 12 (km) from the coast. A system of 2–4 (m) high degraded reticulate dunes. Sampled to 2.5 (m) depth where a hard silty sand surface was encountered.
WK03-6	30.6775°S, 17.6589°E	200	50 (km) SSE of WK03-5, 8.5 (km) N of the Groenrivier, 17 (km) from the coast. Samples the thin (0.2–0.5 (m)) sand mantle covering a low upland similar to that at WK03-3. A sample was taken at 0.4 (m), just above the underlying hard silty sand.
WK03-7	30.7256°S, 17.5719°E	105	11 (km) WSW of WK03-6, 7 (km) N of the Groenrivier, 4 (km) from the coast. Samples a large ~2 (m) thick degraded barchanoid feature. Exceptionally dry sediments resulted in only one undisturbed sample, at 1.5 (m), to be obtained before the core failed.
WK03-8	30.7264°S, 17.5717°E	105	Taken 30 (m) to the south of WK03-7, from the same dune form, WK03 was excavated to a depth of 1 (m) with a spade before coring through to the underlying hard silty sand at 2 (m) depth.
WK03-9	30.7350°S, 17.5717°E	95	Taken from a N–S trending dune form 500 (m) south of WK03-7 and 8. Sampled to a depth of 3 (m) before encountering the underlying hard pan.
WK03-10	30.9703°S, 17.7831°E	150	33 (km) SSE of WK03-7–9, 6 (km) N of the Brakrivier, 10 (km) from the coast. Samples a linear element of a well-developed reticulate dunefield. Core halted at a depth of 1.5 (m) by the underlying hard pan.
WK03-11	30.9697°S, 17.7808°E	145	Samples the sandy mantle in the interdune depression 230 (m) WNW of WK03-10. Excavation with a spade exposed 0.5 (m) of surficial material above a hard silty sand.
WK03-12	30.9692°S, 17.7811°E	150	60 (m) NNE of WK03-11. Extremely dry sediment precluded coring, and a pit was excavated to a depth of 1 (m) with a spade.
WK03-13	30.9711°S, 17.7861°E	140	300 (m) ESE of WK03-10, WK03-13 samples an interdune region, a sample of silty sand similar to that seen at WK03-11 was obtained.
WK03-14	31.1464°S, 17.8728°E	140	21 (km) SSE of WK03-10–13, 5.7 (km) NW of the Soutrivier. Samples a transverse element in a highly degraded dunefield. Unlike at other sites, notable stratigraphic variations were evident within this core. At 1.4 (m) a 2–3 cm thick ferruginous layer was encountered, and at 2.5 (m) sediment colour changed from 7.5 YR 5/4 Brown to 7.5 YR 5/6 Strong brown, though without any significant change in composition or structure. The core bottomed out at 3.5 (m), but no basal sediments were recovered.
WK03-15	31.4992°S, 18.1847°E	95	10 (km) from coast, 9 (km) N of the Olifants River. Southern margin of the regions large (310 sq (km)) reticulate dunefield. Access being limited in the area, this sites samples a 2.75 (m) dune next to the road. Road spoil was removed with a spade and the dune was cored through to the underlying hard pan.
WK03-16	31.9036°S, 18.3872°E	161	48 (km) SSE of WK03-15, 10 (km) from the coast. Taken from a highly degraded aeolian landscape, this cores exhibits distinct stratigraphic variations with significant ferruginous concretions being found below 2.5 (m) and a 2 (cm) thick calcrete being encountered at 3.9 (m). Below this the sediment became siltier, and coring was halted at 4.5 (m).

grain size. Heavy minerals were removed from the sieved samples by density separations at 2.75 g/cm³. Quartz was obtained from the less dense fraction using an HF acid etch (40% HF for 60 min followed by a 30-min HCl rinse) and then re-sieved. Three aliquots of each sample were tested for feldspar contamination using the IR depletion method of Duller [41]. Samples which failed this test were re-etched. Measurements were car-

ried out on a Risø TL-DA-15 computer controlled luminescence reader. For each determination, stimulation was provided by a 150-W halogen lamp, filtered by GG420 long pass and SWP interference filters. Luminescence was measured by a Thorn EMI 9235QA photomultiplier tube filtered through a Hoya U-340 filter. Irradiation was carried out using a calibrated ⁹⁰Sr/⁹⁰Y beta source [42].

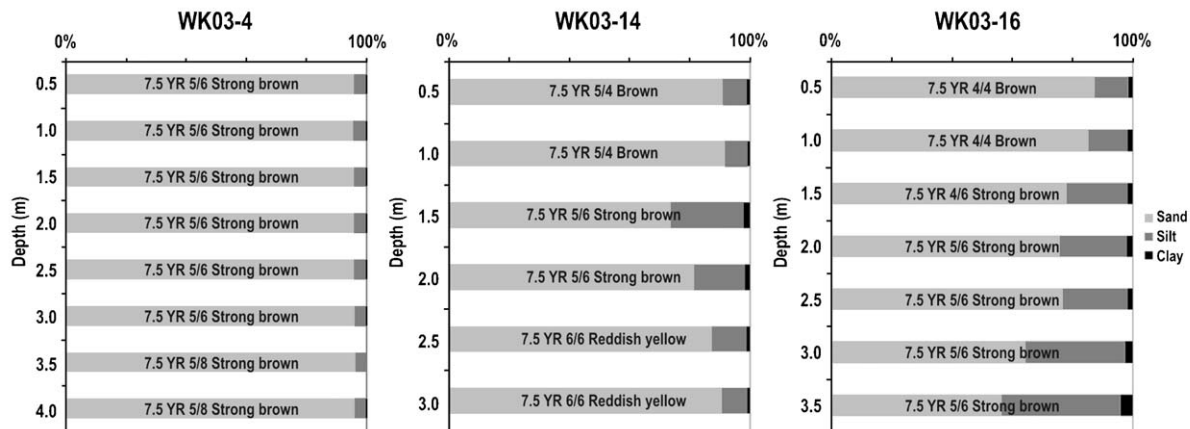


Fig. 3. Comparison of grain size and colour variations from a typical west coast reticulate dune (WK03-4) and WK03-14 and WK03-16.

Prior to OSL measurement, preheat plateau tests (20 °C intervals from 160–300 °C) were conducted on one sample from each site [43]. Preheat temperatures of 220 °C were determined as optimal for samples from sites WK03-4, 12, 14, 15 and 16, while samples from WK03-2, 3, 5, 7, 8, 9, 10, and 13 were preheated to 240 °C. Preheat times for all samples were 10 s, and a 160 °C cutheat was used for all test doses.

Palaeodose determinations were obtained using either a five-point single aliquot regeneration (SAR) protocol [44], or were calculated using a standardised growth curve (SGC) [45]. For SAR measurements, a replicate recycling measurement of the first regeneration point was used to test that sensitivity corrections were being adequately made. Those few aliquots with recycling ratios deviating from unity by greater than 10% were rejected [44]. Growth curves were fitted using a saturating exponential plus linear function in the Luminescence Analyst software [46].

To create the SGC used in this study, 1463 aliquots representing 22 regenerated doses ranging from 0–33 Gy were used. Although Roberts and Duller [45] suggest that samples from different regions can be measured on a single growth curve, studies conducted by Telfer et al. [47] show sufficient inter-regional variability to warrant caution. Considering this, only samples from west coast sites were used to create the SGC used here.

Between 18 and 42 aliquots were measured for each sample, with frequency histograms using objective bin sizing criteria [48] and probability density plots being constructed from a minimum of 18 accepted aliquots. For normally distributed samples, the equivalent dose (D_e) was taken to be the mean weighted by the absolute variance, with errors being calculated as standard errors. Aliquots from some samples lay distinctly beyond the normal distribution of the data set, and were removed

before calculating the weighted mean. This was limited to one to three aliquots per sample, and can be justified statistically with Chauvenet's criterion, which states that measurements with probabilities of less than 1/2 can be rejected [49]. Uncertainties are based on the propagation, in quadrature, of errors associated with individual errors for all measured quantities. In addition to uncertainties calculated from counting statistics, errors due to 1) beta source calibration (3%, [42]), 2) alpha and beta counter calibration (3%), 3) dose rate conversion factors (3%) and 4) attenuation factors (2%) have been included.

3.4. Dose rates

Dose rate calculations were derived from measurements of the concentrations of uranium (U), thorium (Th) and potassium (K) in each sample. These were determined by inductively coupled plasma mass spectrometry (ICP-MS) at the Oxford University Earth Science Department and the Department of Earth Sciences and Geography, Kingston University, and by inductively coupled plasma atomic emission spectrometry (ICP-AES) at the Department of Geology, Royal Holloway College. Blanks were found to be negligible for all the elements measured. The precision of the data ranged from relative standard deviations of 3.2% for U and Th to 3.5% for K. Detection limits were as follows: U (0.0009 ppm), Th (0.0006 ppm), K (0.07%). Concentrations of U, Th and K were converted to a dose rate of Gy/ka using the values in Aitken [50]. As the errors calculated for these concentrations reflect the high precision of the measurements, but not the potential errors associated with the preparation of heterogeneous samples, 15% errors have been applied, based on values reported

Table 2
OSL samples from west coast reticulate dunes, dose rate data, palaeodoses and ages

Site	Lab code	Depth (m)	K (%)	U (ppm)	Th (ppm)	Water Content (%)	Cosmic (Gy/ka)	Dose Rate (Gy/ka)	Bedform	Calculation technique	De (Gy)	Age (ka)
WK03 2-1	Shfd04057	1.0	1.01±0.15	0.88±0.17	4.17±0.03	0.25	0.18±0.009	1.63±0.13	Surficial sand	SAR and SGC	16.9±0.38	10.4±0.93
WK03 3-1	Shfd04058	1.0	1.54±0.23	1.60±0.24	9.62±1.44	5.61	0.18±0.009	2.55±0.20	Surficial sand	SAR	24±0.41	9.40±0.82
WK03 3-2	Shfd04059	1.5	1.87±0.28	1.27±0.19	10.84±1.63	11.85	0.19±0.009	2.66±0.22	Soil	SAR	119±4.5	44.8±4.33
WK03 4-1	Shfd04060	0.5	1.37±0.21	0.34±0.05	1.58±0.24	1.68	0.19±0.010	1.66±0.18	Reticulate dune	SGC	7.23±0.19	4.36±0.49
WK03 4-2	Shfd04061	1.0	1.58±0.24	0.33±0.05	1.81±0.27	0.96	0.18±0.009	1.88±0.20	Reticulate dune	SAR and SGC	8.18±0.17	4.36±0.50
WK03 4-3	Shfd04062	1.5	1.40±0.21	0.41±0.06	2.09±0.31	2.07	0.17±0.009	1.71±0.18	Reticulate dune	SGC	8.9±0.23	5.21±0.57
WK03 4-4	Shfd04063	2.0	1.32±0.20	0.34±0.05	1.70±0.26	2.40	0.17±0.008	1.59±0.17	Reticulate dune	SAR	11.2±0.16	7.04±0.77
WK03 4-5	Shfd04064	2.5	1.39±0.21	0.35±0.05	1.62±0.24	0.11	0.17±0.008	1.68±0.18	Reticulate dune	SGC	12.3±0.27	7.33±0.83
WK03 4-6	Shfd04065	3.0	1.58±0.24	0.30±0.05	1.76±0.26	0.12	0.16±0.008	1.86±0.21	Reticulate dune	SGC	17.1±0.32	9.16±1.06
WK03 4-7	Shfd04066	3.5	1.38±0.21	0.28±0.04	1.67±0.25	0.12	0.16±0.008	1.66±0.18	Reticulate dune	SGC	20.6±0.39	12.4±1.41
WK03 4-8	Shfd04067	4.0	1.78±0.27	0.31±0.05	1.67±0.25	0.13	0.15±0.007	2.04±0.23	Reticulate dune	SGC	25.8±0.79	12.6±1.53
WK03 5-1	Shfd04068	1.0	0.62±0.09	2.15±0.32	30.9±4.64	0.23	0.18±0.009	3.39±0.28	Reticulate dune	SGC	12.9±0.31	3.81±0.35
WK03 5-2	Shfd04069	2.0	0.72±0.11	2.57±0.39	29.3±4.40	2.23	0.16±0.008	3.39±0.27	Reticulate dune	SGC	19.3±0.94	5.68±0.56
WK03 5-3	Shfd04070	2.5	0.73±0.11	2.31±0.35	21.9±3.28	0.22	0.18±0.009	2.96±0.22	Reticulate dune	SGC	45.8±1.57	15.5±1.36
WK03 6-1	Shfd04071	0.4	0.62±0.09	1.92±0.29	22.2±3.33	0.94	0.20±0.010	2.74±0.21	Surficial sand	SAR	11.1±1.86	4.05±0.76
WK03 7-1	Shfd04072	1.0	0.71±0.11	2.21±0.33	20.4±3.06	0.44	0.18±0.009	2.76±0.21	Reticulate dune	SGC	16±0.35	5.79±0.49
WK03 7-2	Shfd04073	1.5	0.73±0.11	1.98±0.30	25.0±3.75	1.13	0.17±0.008	3.01±0.24	Reticulate dune	SGC	22.2±0.46	7.37±0.64
WK03 7-3	Shfd04074	2.0	0.83±0.13	2.48±0.37	22.6±3.39	0.28	0.16±0.008	3.08±0.23	Reticulate dune	SGC	19.3±0.22	6.26±0.52
WK03 8-1	Shfd04075	0.5	0.78±0.12	1.99±0.30	20.3±3.04	0.65	0.19±0.010	2.83±0.21	Reticulate dune	SGC	4.41±0.17	1.56±0.14
WK03 8-2	Shfd04076	1.5	0.95±0.14	5.57±0.84	50.4±7.56	0.34	0.18±0.009	5.83±0.48	Reticulate dune	SAR	100±4.13	17.2±1.65
WK03 9-1	Shfd04078	0.5	0.82±0.12	2.11±0.32	20.7±3.11	1.57	0.19±0.010	2.85±0.21	Reticulate dune	SGC	7.82±0.51	2.74±0.28
WK03 9-2	Shfd04079	1.0	0.85±0.13	2.73±0.41	32.8±4.93	1.64	0.18±0.009	3.82±0.31	Reticulate dune	SGC	11±0.81	2.89±0.33
WK03 9-3	Shfd04080	1.5	0.80±0.12	2.10±0.32	22.1±3.31	1.66	0.18±0.009	2.90±0.22	Reticulate dune	SGC	12.4±0.19	4.27±0.35
WK03 9-4	Shfd04081	2.0	0.81±0.12	2.99±0.45	36.8±5.51	0.77	0.17±0.008	4.14±0.34	Reticulate dune	SGC	20.9±0.26	5.05±0.45
WK03 9-5	Shfd04082	2.5	0.78±0.12	2.86±0.43	32.5±4.88	2.43	0.17±0.008	3.72±0.30	Reticulate dune	SGC	25.3±0.42	6.81±0.60
WK03 9-6	Shfd04083	2.8	0.86±0.13	1.82±0.27	21.9±3.29	0.24	0.19±0.009	2.94±0.23	Reticulate dune	SGC	66.1±1.26	22.5±1.90
WK03 10-1	Shfd04084	0.5	0.21±0.03	0.38±0.06	1.63±0.24	1.77	0.19±0.01	0.59±0.03	Reticulate dune	SGC	4.5±0.26	7.67±0.65
WK03 10-2	Shfd04085	1.0	0.20±0.03	0.43±0.07	1.58±0.24	2.05	0.19±0.009	0.58±0.03	Reticulate dune	SGC	7.39±0.25	12.8±0.92
WK03 10-3	Shfd04086	1.5	0.22±0.03	0.30±0.05	1.60±0.24	0.20	0.18±0.009	0.58±0.03	Reticulate dune	SAR and SGC	13.1±0.33	22.7±1.57
WK03 11-1	Shfd04087	0.5	0.37±0.06	2.46±0.37	11.7±1.75	4.35	0.19±0.01	1.84±0.13	Surficial sand	SGC	23.1±1.17	12.6±1.13
WK03 12-1	Shfd04088	0.5	0.24±0.04	0.72±0.11	2.80±0.42	0.22	0.19±0.01	0.78±0.05	Reticulate dune	SAR and SGC	4.09±0.15	5.24±0.40
WK03 12-2	Shfd04089	1.0	0.22±0.03	0.43±0.06	1.93±0.29	0.16	0.18±0.009	0.63±0.03	Reticulate dune	SAR	7.56±0.35	12.0±0.93
WK03 13-1	Shfd04090	0.2	0.81±0.12	1.32±0.20	13.2±1.98	8.63	0.20±0.01	2.04±0.14	Soil	SAR	49.7±1.22	24.4±1.98
WK03 14-1	Shfd04091	0.5	0.24±0.04	1.09±0.01	2.04±0.31	0.79	0.19±0.01	0.81±0.04	Reticulate dune	SGC	6.31±0.24	7.75±0.54
WK03 14-2	Shfd04092	1.0	0.25±0.04	1.08±0.16	3.46±0.52	0.48	0.18±0.009	0.91±0.05	Reticulate dune	SAR	8.1±0.22	8.93±0.65
WK03 14-3	Shfd04093	1.5	0.32±0.05	1.10±0.09	4.56±0.68	2.70	0.18±0.009	1.02±0.06	Reticulate dune	SGC	14.2±0.51	13.9±1.04
WK03 14-4	Shfd04094	2.0	0.31±0.05	1.10±0.17	5.03±0.75	2.04	0.17±0.008	1.04±0.07	Reticulate dune	SGC	14.7±0.25	14.1±1.03
WK03 14-5	Shfd04095	2.5	0.27±0.04	1.09±0.07	3.24±0.49	1.71	0.17±0.009	0.90±0.05	Reticulate dune	SGC	23.2±0.64	25.9±1.74
WK03 14-6	Shfd04096	3.0	0.20±0.03	1.08±0.16	3.69±0.55	0.82	0.17±0.009	0.87±0.05	Reticulate dune	SGC	36.7±1.11	42.3±3.07
WK03 15-1	Shfd04097	0.5	0.17±0.03	0.28±0.04	1.06±0.16	0.32	0.19±0.01	0.49±0.03	Reticulate dune	SGC	1.1±0.09	2.24±0.24
WK03 15-2	Shfd04098	1.0	0.17±0.03	0.26±0.04	0.93±0.14	0.62	0.19±0.009	0.48±0.03	Reticulate dune	SAR and SGC	3.18±0.08	6.67±0.48
WK03 15-3	Shfd04099	1.5	0.12±0.02	0.20±0.03	0.90±0.14	0.62	0.18±0.009	0.40±0.02	Reticulate dune	SGC	3.53±0.1	8.77±0.59
WK03 15-4	Shfd04100	2.0	0.12±0.02	0.29±0.04	1.08±0.16	0.22	0.18±0.009	0.44±0.03	Reticulate dune	SGC	5.64±0.21	12.9±0.91
WK03 15-5	Shfd04101	2.5	0.14±0.02	0.23±0.03	1.07±0.16	0.26	0.17±0.008	0.42±0.03	Reticulate dune	SAR	5.88±0.13	13.9±0.88
WK03 16-1	Shfd04102	0.5	0.17±0.03	0.67±0.10	3.10±0.46	1.69	0.19±0.01	0.72±0.04	Reticulate dune	SGC	3.05±0.18	4.21±0.37
WK03 16-2	Shfd04103	1.0	0.22±0.03	0.72±0.11	2.62±0.39	3.85	0.19±0.009	0.73±0.04	Reticulate dune	SAR	7.36±0.27	10.0±0.72
WK03 16-3	Shfd04104	1.5	0.29±0.04	0.81±0.12	4.16±0.62	1.24	0.18±0.009	0.92±0.06	Reticulate dune	SGC	9.3±0.33	10.1±0.76
WK03 16-4	Shfd04105	2.0	0.29±0.04	0.86±0.13	2.95±0.44	2.22	0.17±0.009	0.83±0.05	Reticulate dune	SAR	10.7±0.24	12.8±0.89
WK03 16-5	Shfd04106	2.5	0.32±0.05	0.63±0.09	3.41±0.51	2.65	0.16±0.008	0.83±0.05	Reticulate dune	SGC	10.7±0.39	12.9±1.03
WK03 16-6	Shfd04107	3.0	0.47±0.07	0.86±0.13	4.21±0.63	4.68	0.16±0.008	1.07±0.07	Reticulate dune	SGC	17.3±0.43	16.2±1.26
WK03 16-7	Shfd04108	3.5	0.72±0.11	1.31±0.20	5.85±0.88	7.25	0.18±0.009	1.47±0.10	Reticulate dune	SAR	118±2.59	80.4±6.38

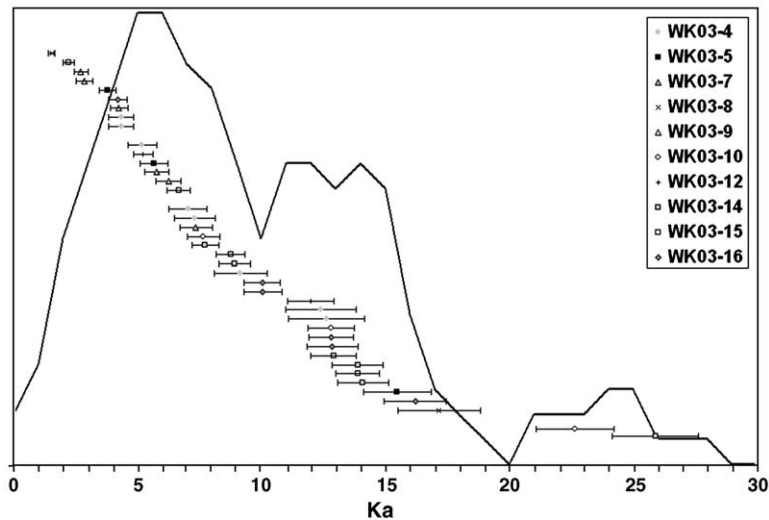


Fig. 4. Age ranked OSL ages from reticulate dune forms from the west coast of South Africa.

for geological standards, and reproducibility tests conducted on samples of dune samples (rather than blanks) for this study. Cosmic dose contributions were calculated based on Prescott and Hutton's [51] algorithm, with the age and depth of overlying units being considered. Palaeomisture values were assumed to be similar to those obtained from the collected samples (ranging from 0.25–14%), with $5 \pm 5\%$ being applied to account for past fluctuations.

3.5. OSL ages from reticulate dunes

OSL age determinations for the study sites are shown schematically (Fig. 1), with the data used to determine ages presented in Table 2. While few ages earlier than 17 ka are preserved in the reticulate dune system, that reticulate dune activity can be identified throughout the Lateglacial and Holocene (Fig. 4). Although several 'statistically distinct phases' exist [c.f. 39], for example at 3.81–4.36, 5.05–7.75, and 8.77–10.1 ka, many are of short duration and in close proximity to neighbouring clusters. These phases may represent sporadic activity in an environment close to the threshold of aeolian transport, or, despite the improved resolution compared to most published luminescence chronologies, they may simply be an artefact of the sampling interval. Highlighted with a 5-point moving average,² three broader

clusters can be identified from the dataset at approximately 4–8, 12–17, and 22–25 ka (Fig. 4).

In the total data set, the ages at 22 ka and earlier represent outliers to the general pattern of Lateglacial–Holocene activity for these dune forms. The limited occurrence of ages corresponding to the last glacial period contrasts with the ages determined from the coversand deposits of the west coast [19]. This pattern of ages is best explained by recourse to the morphology of the dunes. The reticulate pattern has developed from the stabilisation and subsequent reworking of migratory dune forms that do not accumulate sand in a manner that preserves earlier phases of sediment transport. The full and regular recycling of migratory dune bodies means that only the cessation of activity is recorded, with prior periods of dune mobility being systematically erased. From this perspective, the older basal ages obtained from the reticulate dune cores (22.5 ± 1.90 , 22.7 ± 1.57 , 25.9 ± 1.74 , 42.3 ± 3.07 and 80.4 ± 6.38 ka) are most likely not representative of the dunes themselves, but rather aeolian sediments that have been incorporated to some degree into the sediment underlying the dunes, and have, either as a result of groundwater influences or vegetation development, resisted deflation.

3.6. Interdune deposits: surficial sands and soils

It has long been understood [e.g. 40], and recently re-iterated [36] that the thin deposits of sand present in interdune depressions are not necessarily deposited as the result of aeolian activity. While it is possible that

² Given the limited number of samples, this method was chosen in favour of a probability density plot, which requires larger data sets in order to be reliable. Errors were not included in these calculations as the smaller errors associated with younger ages would bias the results.

they may represent temporary sinks for windblown material or exposures of truncated aeolian material [52], they may also have been deposited as a part of the degradation process of the adjacent dunes through sheet wash. Since these deposits could be the result of mechanisms enabled by either humid or arid climate regimes, the inference of a clear palaeoenvironmental signal is complex, if not impossible.

In this study, the interdune sediments sampled for OSL dating consist of surficial sands and deeply weathered granite bedrock soils with varying amounts of allochthonous sediments, primarily aeolian sands. Depending on the rate of soil development versus allochthonous deposition, OSL ages obtained from soils can vary in terms of their quality and palaeoenvironmental significance. If rates of external sediment input are low, it is expected that a range of OSL measurements will be obtained, ranging from the most recent inputs to elements of dose saturated weathered bedrock. If sedimentation rates are sufficiently high, discrete phases of deposition and tight distributions of OSL measurements may be preserved. A broad distribution cannot, however, simply be taken as diagnostic of slow sedimentation rates, as bioturbated sediments may be expected to exhibit similar patterns.

What ages obtained from these deposits may mean in terms of environmental change depends on the dynamics of the system. An episode of high sedimentation within, or followed by, a period of humid conditions conducive to pedogenesis could result in a soil developing on the sediment body. Ages from this soil would not date the humid period during which the soil developed, but the initial depositional episode. If, however, low sedimentation rates existed during generally mesic conditions, it would be possible for pedogenesis and external sediment inputs to keep pace. An age from these deposits would represent the slow accumulation of sediment in a humid to sub-humid environment.

3.6.1. OSL ages from surficial sands and soils

Sites WK03-11 and-13 sample the surficial sands and soil respectively from the reticulate dunefield sampled as WK03-10 and-12. The ages from the reticulate features provide a context within which the ages from the interdune sands and soil can be interpreted. The age of 12.6 ± 1.13 ka from WK03-11 falls within the 12–17 ka peak identified from the aggregate of reticulate ages, as well as the ages of 12.8 ± 0.92 ka and 12.0 ± 0.93 ka obtained from the reticulates at WK03-10 and 12. This suggests that these sediments were deposited towards the end of a phase of widespread aeolian activity.

An age of 24.4 ± 1.98 ka was obtained from the soil at WK03-13, with the OSL measurements exhibiting a tight distribution (Fig. 5), suggesting little mixing of aeolian and bedrock components, and limited bioturbation. To test if younger sediments associated with the phase of widespread reticulate activity from 12–17 ka were incorporated in this unit, an age was calculated from the youngest OSL measurement. This age of 18.1 ± 3.07 ka suggests that the mixing of sediments from this phase of activity is unlikely. Basal reticulate ages from WK03-9 and -10, 22.1 ± 1.90 ka and 22.7 ± 1.57 ka respectively, imply that aeolian activity occurred in the region during this general period, although whether the WK03-13 sediments represent aeolian or sheet wash deposits, or whether soil development occurred during or after deposition is unclear.

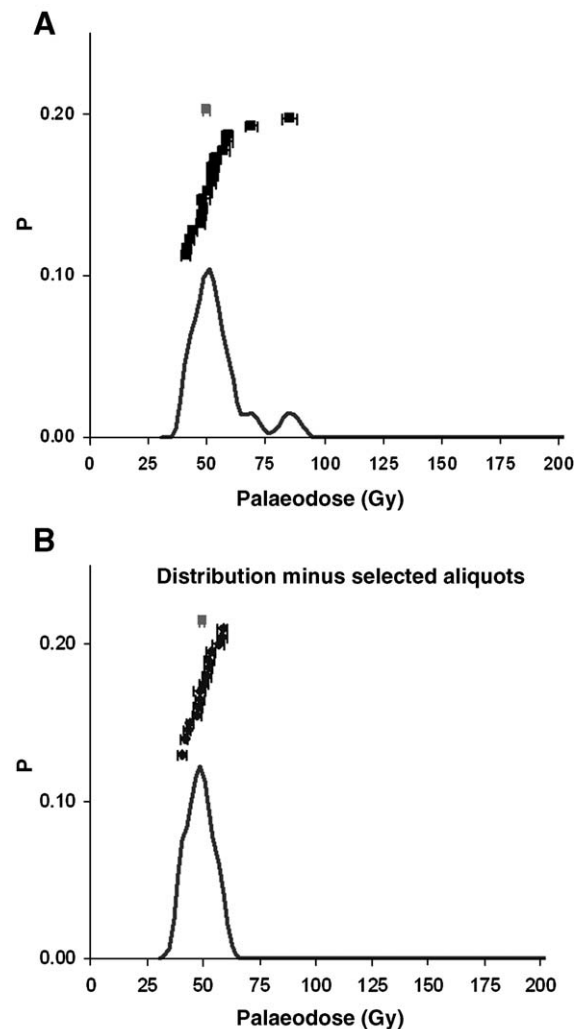


Fig. 5. Distribution of D_e values from OSL age measurements for sample WK03-3-2.

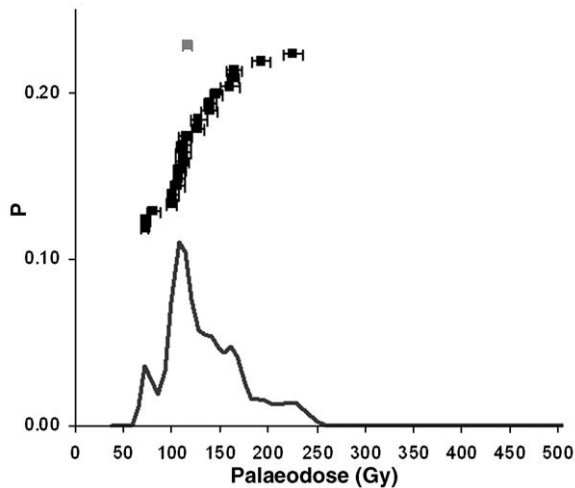


Fig. 6. Distribution of D_e values from OSL age measurements for sample WK03-3-2.

The soil sampled at WK03-3 exhibits a much broader multimodal distribution (Fig. 6) and the obtained age of 44.8 ± 4.33 ka is of questionable value. Ages of aeolian activity of 42.8–48.6 ka from a previous study [19] suggest that this may have been a period of regional activity, but as with the sample from WK03-13, how the “age” relates to periods of pedogenesis or aeolian activity is uncertain.

Although the mechanical action of the auger used for sampling is not conducive to the identification and analysis of high-resolution stratigraphic variations within a core, the sedimentology of the WK03-14 core is

strongly suggestive of the development of a palaeosol at 1.5 m (Fig. 3). Ages from this and neighbouring samples may indicate a period of relative geomorphic stability during the early Holocene from approximately 14–9 ka.

3.6.2. Reticulate form phases

Unlike the phases of aeolian accumulation identified at 4–5, 16–24, 30–33, 43–49 and 63–73 ka in the coversands from the region [19], the reticulate dune forms record phases of accumulation at markedly different times during the late Quaternary (Fig. 7).

Comparing 5-point moving averages of the reticulate dune forms and coversands highlights the broadly inverse relationship between the datasets, and when compared to records of wind strength and fluvial activity from the west coast region (Fig. 8) distinct patterns can be observed between dune forms and these potential forcing mechanisms. While phases of activity/deposition preserved in the accumulating forms correspond with phases of increased wind strength and potentially increased fluvial sediment supply, the primary age clusters from reticulate forms occur *after* both wind strength and fluvial sediment transport drop of sharply in the early Lateglacial.

It is unlikely that the reticulate dunes would actually become more active during a period of relatively high humidity [25,53] and decreased wind and sediment supply, but because OSL ages from dune forms represent only *preserved* phases of accumulation, it is likely that the degraded reticulate features found along the west coast, as migrating features, represent the last

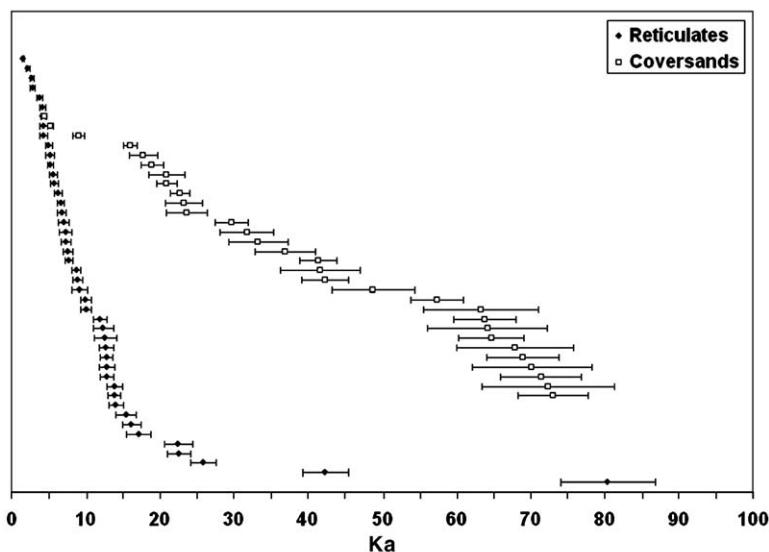


Fig. 7. Age ranked plot of ages from coversands [19] and reticulate dune forms from the west coast of South Africa.

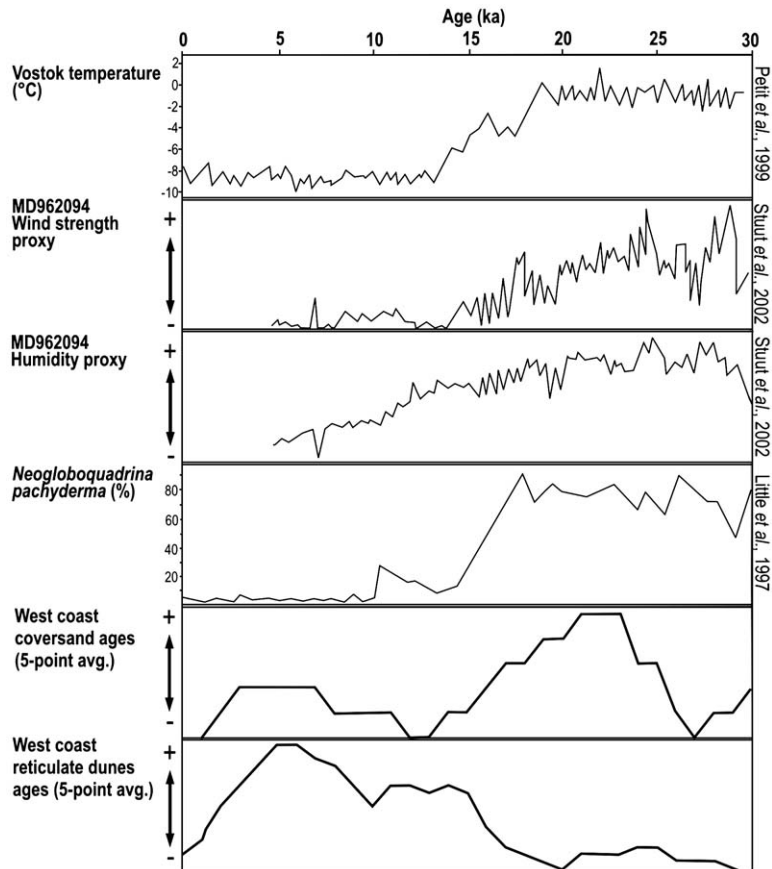


Fig. 8. Comparison of Vostok temperature records [2], proxies for wind strength (ratio of coarse to fine aeolian sediment) and fluvial activity (proportion of hemipelagic sediment) from Namibian marine core MD962094 [13], abundances of foraminifera associated with coastal upwelling/elevated wind strength [14], and 5-point moving averages of the number of OSL ages from reticulate dunes and coversands from the west coast of South Africa.

generation of dunes in what was once a highly dynamic and mobile landscape.

4. Discussion

Based on the OSL ages obtained from the dune forms of the west coast, it appears that the most intense phases of aeolian activity occurred during glacial periods. The thickest aeolian deposits and the cores of some of the region's reticulate dune forms date to Oxygen Isotope Stages (OIS) 2, 3 and 4. Other palaeoenvironmental proxies suggest that these were periods of increased humidity in the region [e.g. 8, 12, 13, 25], and the possibility exists that the west coast's aeolian deposits reflect increased sediment supply from invigorated fluvial sources [e.g. 54]. Increases in humidity, however, covary strongly with increases in windiness and aeolian transport capacity, as indicated by a variety of marine proxies [e.g. 13, 14] (Fig. 8). This close relationship

between precipitation and wind is to be expected, given that Antarctic cooling is predicted to intensify hemispheric circulation cells [e.g. 23], including the South Atlantic Anticyclone that influences the west coast, as well as strengthening and extending the influence of the moisture-bearing westerlies [e.g. 55]. It is therefore more likely that variations in windiness and transport capacity dictate the periodicity of aeolian activity in the region during glacial periods, and that increased fluvial sediment supply plays a supporting role, primarily in increasing the potential for the preservation of aeolian archives.

The Lateglacial was a transitional period along the west coast. Evidence from both marine and terrestrial archives indicate steady declines in windiness and humidity beginning at ~23–20 ka. By 15 ka, while humidity was still significantly greater than it is today [e.g. 11, 12, 25], wind intensities had dropped markedly to low interglacial levels [e.g. 13, 14]. At this time, as

accumulating dune forms along the west coast entered a period of dormancy, and the reticulate dunes became fixed features of the landscape, with geomorphic stability being indicated at WK03-14.

In contrast to the accumulating forms, reticulate dunes, with their distinct crescentic cores, are generally migratory features. As such, when active and mobile they would have regularly recycled their sediments, resetting its luminescence signal over decadal timescales [c.f. 56], and only preserving depositional records once they had become dormant. Therefore, the reticulate dune form ages along the west coast do not indicate aeolian “activity”, but rather a decline in transport capacity as hemispheric circulation cells weakened during the glacial–interglacial transition.

Preserved within the reticulate dunes are three distinct suites of ages, each with fundamentally different controls. During periods of increased wind strength, mobile crescentic forms would have moved rapidly across the west coast’s interior plateau. The interaction between an active aeolian system and what appears to have been a more humid climate [e.g. 12,25] would have resulted in the development of a landscape of migratory forms centred on, or temporarily anchored by nebkhas that acted as dune nuclei, and are visible in the modern landscape (Fig. 2). Ages at 22.5 ± 1.90 , 22.7 ± 1.57 , 25.9 ± 1.74 , 42.3 ± 3.07 and 80.4 ± 6.38 ka may relate to such features. Similar ages obtained from soils at WK03-3 and WK03-13 are further suggestive of a system in which relatively humid conditions facilitated the incorporation of aeolian sediments into the region’s substrate. These nebkha deposits would have been preserved when, buried by the development of ephemeral crescentic dunes, the wind intensity along the west coast decreased sharply across the last glacial transition, and the dunes became fixed landscape features between 12–17 ka. Increased humidity in the region, though declining, persisted until approximately 10 ka, when xeric thicket taxa first appear at Elands Bay Cave [25], and indications of dune field remobilisation begin to appear (Fig. 8).

The Holocene along the west coast is characterised by progressively drier conditions and significantly reduced wind speeds compared to OIS 2, 3 and 4 [13,14,57]. The warmest portion of the Holocene, the HA (~4–8 ka), also appears the driest, with high percentages of xeric taxa being recorded in the region’s palaeoecological archives [25,58–60]. During the HA, significant widespread dunefield activity and reorganisation is apparent along the whole of the west coast. This reactivity appears in both accumulating and reticulate dune forms (Fig. 8); probably occurring in the form of deflation hollows and

parabolic dunes in the former, and resulting in the elongation and development of linear elements in the latter, though a more spatially intense dating programme would be required to confirm this. Almost certainly not the result of increased windiness, this phase of activity could possibly have been the result of pulses of sediment forced onshore by mid-Holocene high sea levels [e.g. 61]. However, the ubiquity of deposits dating to this period, and the lack of a clear pattern between the timing of deposition and the distance of the sites from the coast suggests that marine transgressions were not generally responsible for these phases of activity. Instead, it is proposed that increased aridity and drought-stress reduced vegetation cover to the extent that the seasonally strong winds associated with the South Atlantic Anticyclone and/or Berg wind systems could reactivate and rework the upper 1–2 m of the region’s dormant aeolian deposits.

5. Conclusion

With the exception of the episode of mid-Holocene activity/deposition, increased aridity is not indicated as being the primary driver of either accumulating or reticulate dunefield development along the west coast of South Africa. This stands in direct contrast to the models suggested by researchers such as Stokes and colleagues [26,39] and O’Connor [62] who emphasise the role of increased aridity to the virtual exclusion of other possible forcing mechanisms. It could be suggested that in the presently more humid regions of the Kalahari where these studies took place, a significant reduction in precipitation would be required for aeolian activity to occur. However, the data presented here indicates that conditions along the west coast during phases of dunefield development were most likely more humid [e.g. 25,59,60], and less seasonal [25] than those Kalahari study sites today. Although it is recognised that most of the world’s presently active dunefields exist in areas that receive <200–250 mm of annual rainfall [52,63], aeolian activity can occur in regions that receive >2000 mm of rain per year [e.g. 64]. This occurs today almost exclusively in coastal environments where there is sufficient wind and sediment supply. As phases of the last glacial period are thought to have been significantly windier [e.g. 65,66], the possibility that aeolian activity could have occurred in continental settings as a result of factors other than simply aridity [e.g. 67] should be more carefully considered.

The analysis of a variety of dune forms, and the consideration of their differing specific controls, has allowed for a detailed reconstruction of aeolian sediment

activity along the west coast, and a more complete interpretation of its palaeoenvironmental significance. The comparison of these data with other palaeoenvironmental proxies from the region has provided a vital context for these analyses, and in turn the OSL ages presented provide information from a terrestrial archive for the evaluation and enhancement of conceptual models of long-term environmental change.

Acknowledgements

Partial funding for this project was made available through the Overseas Research Students Award Scheme, and from NERC grants that provided for ICP analyses at the Department of Earth Sciences and Geography, Kingston University and the Department of Geology, Royal Holloway College. Further funding and significant support for this project was provided by Prof. Michael E. Meadows and the Department of Environmental and Geographical Science at the University of Cape Town. As director of the luminescence lab at the University of Sheffield where many of the reported luminescence measurements were carried out, we would like to thank Mark Bateman for his assistance. We would also like to thank Andy Carr, Jan Berend-Stuut and an anonymous reviewer for reviewing the manuscript, and providing valuable criticism and advice.

References

- [1] T.C. Partridge, L. Scott, R. Schneider, Between Agulhas and Benguela: responses of southern African climates of the Late Pleistocene to current fluxes, orbital precession and the extent of the circum-Antarctic vortex, in: R.W. Battarbee (Ed.), *Past Climate Variability through Europe and Africa*, Springer, Dordrecht, Netherlands, 2004.
- [2] J.R. Petit, J. Jouzel, D. Raynaud, N.I. Barkov, J.M. Barnola, I. Basile, M. Bender, J. Chappellaz, M. Davis, G. Delaygue, M. Delmotte, V.M. Kotlyakov, M. Legrand, V.Y. Lipenkov, C. Lorius, L. Pepin, C. Ritz, E. Saltzman, M. Stievenard, Climate and atmospheric history of the past 420,000 yrs from the Vostok ice core, Antarctica, *Nature* 399 (6735) (1999) 429–436.
- [3] M. Stute, A.S. Talma, Glacial temperatures and moisture transport regimes reconstructed from noble gas and $\delta^{18}\text{O}$, Stampriet aquifer, Namibia, *Isotope Techniques in the Study of Past and Current Environmental Changes in the Hydrosphere and the Atmosphere*. IAEA Vienna Symposium 1997 SM-349/53, Vienna, 1998, pp. 307–328.
- [4] M.J. Cockcroft, M.J. Wilkinson, P.D. Tyson, The application of a present-day climatic model to the late Quaternary in southern Africa, *Clim. Change* 10 (2) (1987) 161–181.
- [5] J.E. Parkington, Coastal settlement between the mouth of the Berg and Olifants Rivers, Cape Province, *S. Afr. Archaeol. Bull.* 31 (1976) 127–140.
- [6] R.M. Cowling, C.R. Cartwright, J.E. Parkington, J.C. Allsopp, Fossil wood charcoal assemblages from Elands Bay Cave, South Africa: implications for late Quaternary vegetation and climates in the winter-rainfall fynbos biome, *J. Biogeogr.* 26 (2) (1999) 367–378.
- [7] L. Scott, Palynology of Late Pleistocene hyrax middens, southwestern Cape Province, South Africa: a preliminary report, *Hist. Biol.* 9 (1–2) (1994) 71–81.
- [8] L. Scott, E. Marais, G.A. Brook, Fossil hyrax dung and evidence of Late Pleistocene and Holocene vegetation types in the Namib Desert, *J. Quat. Sci.* 19 (2004) 829–832.
- [9] J.C. Vogel, Isotopic evidence for past climates and vegetation of South Africa, Bothalia (14) (1983) 391–394.
- [10] A.S. Carr, D.S.G. Thomas, M.D. Bateman, M.E. Meadows and B. Chase, Late Quaternary palaeoenvironments of the winter-rainfall zone of southern Africa: palynological and sedimentological evidence from the Agulhas Plain, *Palaeogeogr. Palaeoclimatol. Palaeoecol.* 239, 147–165.
- [11] N. Shi, L.M. Dupont, H.-J. Beug, R. Schneider, Correlation between vegetation in southwestern Africa and oceanic upwelling in the past 21,000 yrs. *Quat. Res.* 54 (2000) 72–80.
- [12] N. Shi, R. Schneider, H.-J. Beug, L.M. Dupont, Southeast trade wind variations during the last 135 kyr: evidence from pollen spectra in eastern South Atlantic sediments, *Earth Planet. Sci. Lett.* 187 (3–4) (2001) 311–321.
- [13] J.-B.W. Stuut, M.A. Prins, R.R. Schneider, G.J. Weltje, J.H.F. Jansen, G. Postma, A 300 kyr record of aridity and wind strength in southwestern Africa: inferences from grain-size distributions of sediments on Walvis Ridge, SE Atlantic, *Mar. Geol.* 180 (1–4) (2002) 221–233.
- [14] M.G. Little, R.R. Schneider, D. Kroon, B. Price, T. Bickert, G. Wefer, Rapid palaeoceanographic changes in the Benguela Upwelling System for the last 160,000 yrs as indicated by abundances of planktonic Foraminifera, *Palaeogeogr. Palaeoclimatol. Palaeoecol.* 130 (1–4) (1997) 135–161.
- [15] B. Eitel, A. Kadereit, W.D. Blümel, K. Hüser, B. Kromer, The Amspoor Silts, northern Namib Desert (Namibia): formation, age and palaeoclimatic evidence of river-end deposits, *Geomorphology* 64 (3–4) (2005) 299–314.
- [16] P. Srivastava, G.A. Brook, E. Marais, Depositional environment and luminescence chronology of the Hoarusib River Clay Castles sediments, northern Namib Desert, Namibia, *Catena* 59 (2) (2005) 187–204.
- [17] K. Heine, Climate change over the past 135 000 yrs in the Namib Desert (Namibia) derived from proxy data, *Palaeoecol. Afr.* 25 (1998) 171–198.
- [18] N. Lancaster, How dry was dry?: Late Pleistocene palaeoclimates in the Namib Desert, *Quat. Sci. Rev.* 21 (7) (2002) 769–782.
- [19] B. Chase and D.S.G. Thomas, Multiphase late Quaternary aeolian sediment accumulation in western South Africa: timing and relationship to palaeoclimatic changes inferred from the marine record, *Quat. Int.* (in press).
- [20] M.E. Marker, P.J. Holmes, The distribution and environmental implications of coversand deposits in the Southern Cape, South Africa, *S. Afr. J. Geol.* 105 (2) (2002) 135–146.
- [21] M.D. Bateman, J.B. Murton, W. Crowe, Late Devensian and Holocene depositional environments associated with the coversand around Caistor, North Lincolnshire, UK, *Boreas* 9 (2000) 1–15.
- [22] M.D. Bateman, The origin and age of coversand in North Lincolnshire, UK, *Permafrost. Periglacial Process.* 9 (1998) 313–325.
- [23] S.E. Nicholson, H. Flohn, African environmental and climatic changes and general atmospheric circulation in the Late Pleistocene and Holocene, *Clim. Change* 2 (1980) 313–348.

- [24] S.P. Harrison, S.E. Metcalfe, F.A. Street-Perrott, A.B. Pittock, C.N. Roberts, M.J. Salinger, A climatic model of the last glacial–interglacial transition based on palaeotemperature and palaeohydrological evidence, in: J.C. Vogel (Ed.), *Late Cainozoic Palaeoclimates of the Southern Hemisphere*, Balkema, Rotterdam, 1984, pp. 21–34.
- [25] J. Parkington, C. Cartwright, R.M. Cowling, A. Baxter, M. Meadows, Palaeovegetation at the Last Glacial Maximum in the Western Cape, South Africa: wood charcoal and pollen evidence from Elands Bay Cave South African, *J. Sci.* 96 (11–12) (2000) 543–546.
- [26] S. Stokes, D.S.G. Thomas, R. Washington, Multiple episodes of aridity in southern Africa since the last interglacial period, *Nature* 388 (6638) (1997) 154–158.
- [27] K. Munyikwa, Synchrony of Southern Hemisphere Late Pleistocene arid episodes: a review of luminescence chronologies from arid aeolian landscapes south of the Equator, *Quat. Sci. Rev.* 24 (23–24) (2005) 2555–2583.
- [28] D.S.G. Thomas, P.W. O'Connor, M.D. Bateman, P.A. Shaw, S. Stokes, D.J. Nash, Dune activity as a record of late Quaternary aridity in the Northern Kalahari: new evidence from northern Namibia interpreted in the context of regional arid and humid chronologies, *Palaeogeogr. Palaeoclimatol. Palaeoecol.* 156 (3–4) (2000) 243–259.
- [29] D.S.G. Thomas, S. Stokes, P.W. O'Connor, Late Quaternary aridity in the southwestern Kalahari Desert: new contributions from OSL dating of aeolian deposits, northern Cape Province, South Africa, *Quaternary Deserts and Climatic Change*, Balkema, 1998.
- [30] D.S.G. Thomas, Desert dune activity: concepts and significance, *J. Arid Environ.* 22 (1) (1992) 31–38.
- [31] N. Lancaster, *The Namib Sand Sea: Dune Forms, Processes and Sediments*, Balkema, Rotterdam, 1989.
- [32] J. Pether, D.L. Roberts, J.D. Ward, Deposits of the West Coast, in: T.C. Partridge, R.R. Maud (Eds.), *The Cenozoic of Southern Africa*, Oxford University Press, 2000, pp. 41–46.
- [33] D.J.L. Visser, Explanation of the 1:1000000 geological map, fourth edition, 1984: the geology of the Republics of South Africa, Transkei, Bophuthatswana, Venda, and Ciskei and the kingdoms of Lesotho and Swaziland, Department of Mineral and Energy Affairs, Republic of South Africa Geological Survey, Pretoria, 1989.
- [34] H. Tsoar, The formation of seif dunes from barchans — a discussion, *Z. Geomorphol.* 28 (1) (1984) 99–103.
- [35] R.A. Bagnold, *The Physics of Blown Sand and Desert Dunes*, Chapman and Hall, London, 1954.
- [36] M.J. McFarlane, F.D. Eckardt, S. Ringrose, S.H. Coetzee, J.R. Kuhn, Degradation of linear dunes in Northwest Ngamiland, Botswana and the implications for luminescence dating of periods of aridity, *Quat. Int.* 135 (1) (2005) 83–90.
- [37] S. Stokes, D.S.G. Thomas, P.A. Shaw, New chronological evidence for the nature and timing of linear dune development in the southwest Kalahari Desert, *Geomorphology* 20 (1–2) (1997) 81–93.
- [38] P.W. O'Connor, D.S.G. Thomas, The timing and environmental significance of late Quaternary linear dune development in western Zambia, *Quat. Res.* 52 (1) (1999) 44–55.
- [39] S. Stokes, G. Haynes, D.S.G. Thomas, J.L. Horrocks, M. Higginson, M. Malifa, Punctuated aridity in southern Africa during the last glacial cycle: the chronology of linear dune construction in the northeastern Kalahari, *Palaeogeogr. Palaeoclimatol. Palaeoecol.* 137 (3–4) (1998) 305–322.
- [40] R.F. Flint, G. Bond, Pleistocene sand ridges and pans in western Rhodesia, *Bull. Geol. Soc. Am.* 79 (1968) 299–313.
- [41] G.A.T. Duller, Distinguishing quartz and feldspar in single grain luminescence measurements, *Radiat. Meas.* 37 (2) (2003) 161–165.
- [42] S.J. Armitage, R.M. Bailey, The measured dependence of laboratory beta dose rates on sample grain size, *Radiat. Meas.* 39 (2) (2005) 123–127.
- [43] S.J. Armitage, G.A.T. Duller, A.G. Wintle, Quartz from southern Africa: sensitivity changes as a result of thermal pre-treatment, *Radiat. Meas.* 32 (5–6) (2000) 571–577.
- [44] A.S. Murray, A.G. Wintle, Luminescence dating of quartz using an improved single-aliquot regenerative-dose protocol, *Radiat. Meas.* 32 (1) (2000) 57–73.
- [45] H.M. Roberts, G.A.T. Duller, Standardised growth curves for optical dating of sediment using multiple-grain aliquots, *Radiat. Meas.* 38 (2) (2004) 241–252.
- [46] G.A.T. Duller, *Luminescence Analyst*, University of Wales, Aberystwyth, 2001.
- [47] M. Telfer, M.D. Bateman, A. Carr, B.M. Chase, D.S.G. Thomas, Application of Standardised Growth Curve (SGC) techniques to a high-resolution study of late Quaternary aeolian dynamics in the southwestern Kalahari, South Africa, *UK Luminescence and ESR Meeting Abstracts and Programme*, University of St. Andrews, 2004.
- [48] K. Lepper, N.A. Larsen, S.W.S. McKeever, Equivalent dose distribution analysis of Holocene aeolian and fluvial quartz sands from Central Oklahoma, *Radiat. Meas.* 32 (5–6) (2000) 603–608.
- [49] J.R. Taylor, *Error Analysis: The Study of Uncertainties in Physical Measurements*, University Science Books, Sausalito, 1977, 327 pp.
- [50] M.J. Aitken, *Thermoluminescence Dating*, Academic Press, London and New York, 1985, 359 pp.
- [51] J.R. Prescott, J.T. Hutton, Cosmic ray contributions to dose rates for luminescence and ESR dating: large depths and long-term variations, *Radiat. Meas.* 23 (1994) 497–500.
- [52] K. Pye, H. Tsoar, *Aeolian Sand and Sand Dunes*, Unwin Hyman, London, 1990.
- [53] M.E. Meadows, A.J. Baxter, Late Quaternary palaeoenvironments of the southwestern Cape, South Africa: a regional synthesis, *Quat. Int.* 57–58 (1999) 193–206.
- [54] H.M. Rendell, M.L. Clarke, A. Warren, A. Chappell, The timing of climbing dune formation in southwestern Niger: fluvio–aeolian interactions and the role of sand supply, *Quat. Sci. Rev.* 22 (10–13) (2003) 1059–1065.
- [55] J.-B.W. Stuut, X. Crosta, K. Van der Borg, R.R. Schneider, On the relationship between Antarctic sea ice and southwestern African climate during the late Quaternary, *Geology* (2004) 909–912.
- [56] P. Felix-Henningsen, A.W. Kandel, N.J. Conrad, The significance of calcretes and palaeosols on ancient dunes of the Western Cape, South Africa, as stratigraphic markers and palaeoenvironmental indicators, in: G. Füleky (Ed.), *1st International Conference on Archaeology and Soils*, BAR International, 2003, pp. 1–15, S1163.
- [57] L. Pichevin, M. Cremer, J. Giraudeau, P. Bertrand, A 190 kyr record of lithogenic grain-size on the Namibian slope: forging a tight link between past wind-strength and coastal upwelling dynamics, *Mar. Geol.* 218 (1–4) (2005) 81–96.
- [58] M.E. Meadows, A.J. Baxter, J. Parkington, Late Holocene environments at Verlorenvlei, Western Cape Province, South Africa, *Quat. Int.* 33 (1996) 81–95.
- [59] R.G. Klein, Size variation in the Cape dune molerat (*Bathyergues suillus*) and late Quaternary climatic change in the southwestern Cape Province, South Africa, *Quat. Res.* 36 (1991) 243–256.

- [60] R.G. Klein, K. Cruz-Urbe, Large mammal and tortoise bones from Elands Bay Cave and nearby sites, western Cape Province, South Africa, in: J. Parkington, M. Hall (Eds.), *Papers in the Prehistory of the Western Cape*, British Archaeological Reports International Series, vol. 332 (1), Archaeopress, Oxford, 1987, pp. 132–163.
- [61] G. Franceschini, *Geology of Aeolian and Marine Deposits in the Saldanha Bay Region, Western Cape, South Africa*, PhD, University of Cape Town, 2003.
- [62] P.W. O'Connor, *Aeolian activity and environmental change in the central Mega Kalahari: implications for the timing, nature and causes of late Quaternary aridity*, PhD, University of Sheffield, 1997.
- [63] N. Lancaster, *Geomorphology of Desert Dunes*, Routledge, London, 1995, 290 pp.
- [64] K. Pye, Morphological development of coastal dunes in a humid tropical environment, Cape Bedford and Cape Flattery, North Queensland, *Geogr. Ann., Ser. A* 64 (1982) 213–227.
- [65] A.B.G. Bush, A comparison of simulated monsoon circulations and snow accumulation in Asia during the mid-Holocene and at the Last Glacial Maximum, *Glob. Planet. Change* 32 (4) (2002) 331–347.
- [66] H. Kawahata, T. Okamoto, E. Matsumoto, H. Ujiie, Fluctuations of aeolian flux and aeolian productivity in the mid-latitude North Pacific during the last 200 kyr, *Quat. Sci. Rev.* 19 (2000) 1279–1291.
- [67] N.F. Alley, Cainozoic stratigraphy, palaeoenvironments and geological evolution of the Lake Eyre Basin, *Palaeogeogr. Palaeoclimatol. Palaeoecol.* 144 (3–4) (1998) 239–263.